

Testing of Materials and Coatings at up to 1150 °C and 300 bar for use in Oxy-Combustion Turbine

Florent Bocher
Senior Research Engineer
Southwest Research Institute
San Antonio, TX, USA

Michael Marshall
Research Engineer
Southwest Research Institute
San Antonio, TX, USA

Elizabeth Trillo
Principal Engineer
Southwest Research Institute
San Antonio, TX, USA

Jeffrey Moore
Institute Engineer
Southwest Research Institute
San Antonio, TX, USA



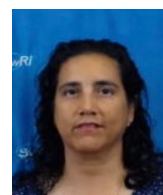
Dr. Florent Bocher is a Senior Research Engineer at Southwest Research Institute in San Antonio, Texas. He has a “Diplôme d’Ingénieur” in materials engineering from ESSTIN, France (now École Polytechnique de l’Université de Lorraine) and a Ph.D. in Materials Science from Imperial College, UK. He specializes in studying environmental performance of materials, including corrosion of metallic alloys and degradation of elastomers and polymers. He has led dozens of R&D projects on evaluating materials in high-temperature and/or high-pressure environments found in various industries such as nuclear power generation, upstream oil and gas, biofuel refinement, hydrogen diffusion, energy generation, and chemical processes.



Michael Marshall is a Research Engineer in the Machinery Department at Southwest Research Institute, where he has conducted work on a range of sCO₂ power cycle applications. He earned his Bachelors in Aerospace Engineering in 2018 from the University of Virginia. His experience includes experimental heat transfer testing, turbomachine and heat exchanger design, root cause failure analysis, and thermodynamic cycle modeling.



Dr. Jeffrey Moore is an Institute Engineer in the Machinery Section at Southwest Research Institute in San Antonio, TX. He holds a B.S., M.S., and Ph.D. in Mechanical Engineering from Texas A&M University. His professional experience over the last 30 years includes engineering and management responsibilities related to centrifugal compressors and gas turbines at Solar Turbines Inc. in San Diego, CA, Dresser-Rand (now Siemens Energy) in Olean, NY, and Southwest Research Institute in San Antonio, TX. His interests include advanced power cycles and compression methods, rotordynamics, seals and bearings, computational fluid dynamics, finite element analysis, machine design, controls, aerodynamics, and oxy-combustion. He has authored over 40 technical papers related to turbomachinery and has four patents issued. Dr. Moore has held positions as the Vanguard Chair of the Structures and Dynamics Committee and Chair of Oil and Gas Committee for IGTI Turbo Expo. He has also served as the Associate Editor for the Journal of Tribology and a member of the IGTI sCO₂ Committee, Turbomachinery Symposium Advisory Committee, the IFToMM International Rotordynamics Conference Committee, and the API 616 and 684 Task Forces.



Dr. Trillo is a Principal Engineer in the Materials Department of the Mechanical Engineering Division at Southwest Research Institute in San Antonio, Texas. She holds a B.S. and M.S. in Metallurgical and Materials Engineering, and a Ph.D. in Materials Science and

Engineering from the University of Texas at El Paso. She has experience in high temperature and high pressure testing (those environments containing H₂S and CO₂), materials evaluation and selection, hydrogen embrittlement, stress corrosion cracking, sulfide stress cracking, general and localized corrosion, and failure analysis. She is actively involved in the development and maintenance of industry standards on hydrogen induced stress cracking (AMPP TM0198), slow strain rate testing in ethanol-based solutions (AMPP TM0111), materials for use in H₂S-containing oil and gas environment (ISO 15156), and the upcoming AMPP technical report on corrosion cracking and fatigue of additively manufactured parts. Dr. Trillo has authored/coauthored 66 technical journal publications.

ABSTRACT

Various materials that may be used in a supercritical carbon dioxide (sCO₂) oxy-fuel turbine in the 150-300 MWe size range are being evaluated in various environments of interest. The inlet of the turbine must be capable of 1,150 °C at 300 bar and the exhaust temperature is expected to be within the 725-775 °C range. The design requirements are pushing the known limits of high temperature materials. Little is known about the oxidation of the metallic alloys considered for turbine nozzles and blades or about the resilience of thermal management solutions, such as thermal barrier coatings (TBC), required to accommodate these high temperatures. The combinations of high temperature resistant materials and coatings must be tested in sCO₂ to evaluate their reliability in an oxy-fuel turbine environment.

A total of 13 alloys were chosen to be tested. They included bare samples, with nano deposited MCrAlY bond coat only, or with the addition of a TBC. A unique test facility was developed to expose those materials in sCO₂ at up to 300 bar and 1150 °C for up to 5,000 hours. This was accomplished by placing an induction heater inside an autoclave to achieve those high temperature locally while the pressurized vessel is cooled externally. The specimens are weighed before and after exposure to determine the oxidation rate. The integrity, morphology, and composition of some of the coatings and thermally grown oxide will be investigated by scanning electron microscopy (SEM).

This paper presents the up-to-date results of the testing coated and uncoated superalloys in sCO₂ at up to 1150 °C and up to 300 bar performed at Southwest Research Institute.

INTRODUCTION

Project Background

Competitive plant efficiencies may be achieved using direct-fired sCO₂ power cycles featuring oxy-combustion, making it an attractive technology. These cycles may also be capable of near zero CO₂ emissions. Past system studies on the Allam-Fetvedt cycle predicted a 53% LHV net efficiency for a plant utilizing natural gas,¹ and a 42% LHV net efficiency for a plant utilizing coal syngas fuel.²

The oxy-combustion systems rely on turbines with inlet temperatures exceeding 1,100 °C. The design undertaken as part of the project sponsored by the U.S. Department of Energy (FE-0031929) includes a six-stage turbine with an input temperature of 1,150 °C at nearly 300 bar.³ A schematic of the turbine and the design temperatures and pressures are presented in Figure 1. As part of this project the various materials considered for the turbine are being evaluated in CO₂ at up to 1,150 °C. The materials evaluation process includes thermal cycling at ambient

pressure CO₂ and long term autoclave testing in high pressure and high temperature sCO₂. Oxidation and thermal management coatings are also included in the experimental matrix.

The materials decision and presentation of the long term autoclave testing facility are presented in this paper along with some of the up-to-date achievements and design optimization.

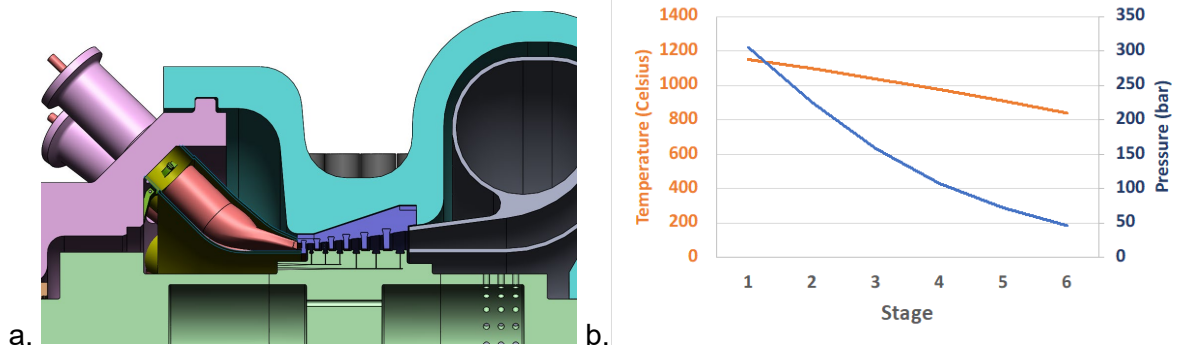


Figure 1. a. Schematic of the six-stage turbine and b. design pressures and temperatures across the stages.

RESULTS AND DISCUSSION

Materials and Specimens

A total of thirteen alloys are included in this study. They cover a wide range of alloys being considered for this application and include baseline alloys that have been evaluated in supercritical CO₂ in multiple studies.⁴⁻¹³ All alloys are exposed with or without a nanocrystalline MCrAlY bond coat. Three of the alloys (740H, 282, and 625) will also be tested with nanocrystalline bond coat and TBC or with a thermal spray bond coat and TBC. The TBC was an yttria-stabilized zirconia-based coating. The list of materials, UNS number, description, and their treatments are summarized in Table 1.

The specimens were machined to a dimension of approximately 1 cm × 1 cm × 0.15 cm, with two 1.5 mm holes. The specimens were coated after machining. Photographs of coated and uncoated 282 specimens are showed in Figure 2 as an example. The nanocrystalline bond coat is approximately 50 μm thick and thus difficult to visually observe. However, specimens are visibly thicker after applying the thermal barrier coating, which is white and has a porous appearance. All specimens were measured (down to 10⁻⁴ inch), photographed, and weighed three times down to 0.1 mg. They will be photographed and weighed after each interruption.

Table 1. List of alloys included in the study, with their UNS number and description. Quantity of each alloy either bare, with a nanocrystalline bond coat alone (NC BC), a nanocrystalline bond coat and thermal barrier coating (NC BC & TBC), or a thermal spray bond coat and thermal barrier coating (TS BC & TBC). Mass change analysis will be performed on all specimens. Additionally, SEM will be performed on the specimens with TBC.

Alloy	UNS	Description	Bare	NC BC	NC BC & TBC	TS BC & TBC
693	N06693	Moderate age-hardened, alumina-former nickel alloy	3	3		
740H	N07740	Age hardened chromia former nickel alloy	3	3	5	5
Nimonic 105	N13021	Age hardened, alumina former nickel alloy	3	3		
APMT Kanthal	n/a	Dispersion strengthened ferritic iron-chromium-aluminum alloy	3	3		
353 MA	S35315	Austenitic, chromium-nickel stainless steel	3	3		
Sanicro 25	S31035	Austenitic 22Cr25NiWCoCu stainless steel	3	3		
718	N07718	High-strength, corrosion-resistant chromia former nickel alloy	3	3		
230	N06230	High strength chromia former nickel alloy	3	3		
625	N06625	Baseline nickel-chromium alloy	3	3	5	5
HR-224	n/a	Alumina former fabricable nickel alloy	3	3		
HR-120	N08120	Solution-strengthened chromia former nickel alloy	3	3		
214	N07214	Nickel-chromium-aluminum-iron alloy	3	3		
282	N07208	Wrought, gamma-prime strengthened nickel superalloy	3	3	5	5

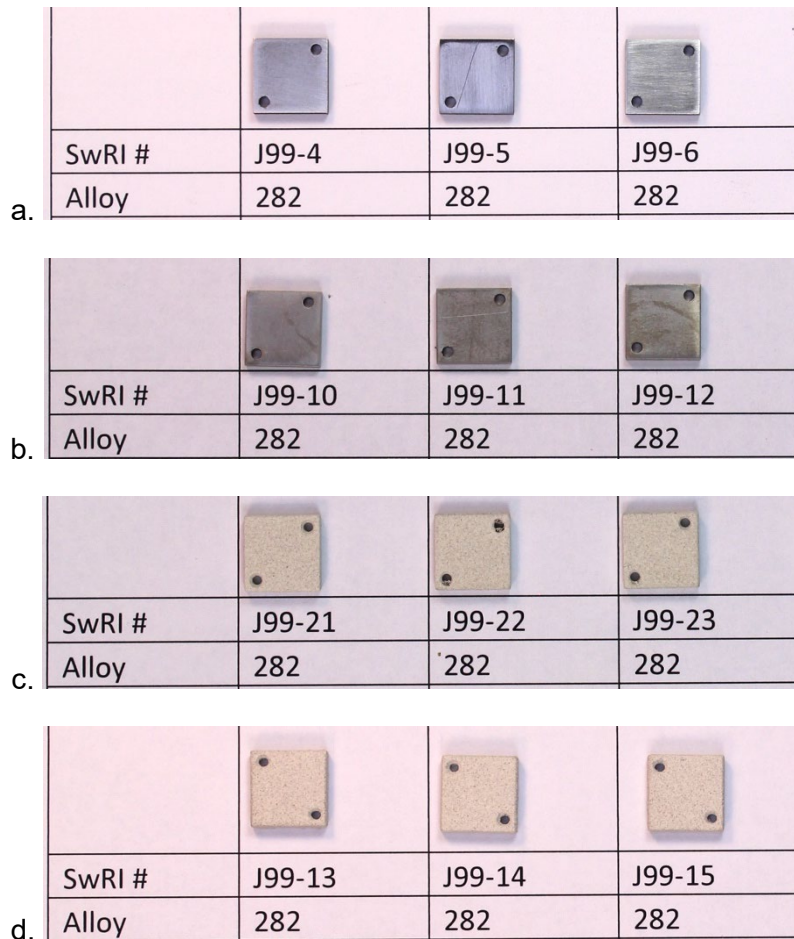


Figure 2. Photographs before exposure of alloy 282 specimens a. bare, b. with nanocrystalline MCrAlY bond coat, c. with nanocrystalline MCrAlY bond coat and TBC, and d. with thermal sprayed bond coat and TBC.

Testing Facility

The unique testing chamber was designed to dissociate the heating source from the pressurized vessel to test materials at 1,150 °C and 300 bar. It is different from traditional methods where the vessel is heated externally using electrical heaters or furnace. Heating inside a cooled autoclave meant that it would be possible to achieve temperatures above 1,000 C locally without being limited by the drop in pressure ratings of commercial autoclaves at high temperature.

A commercially available induction heating system was combined with a stainless steel autoclave rated at 5,000 psi at 350 °C. A schematic of the cross section of the system is shown in Figure 3. The coil path was connected using brass fittings to reinforce copper tubes passing through insulated high pressure and high temperature fittings. The fittings were attached to the head of the autoclave. The coil was attached with brass fittings to those tubes on the inside of the autoclave. The autoclave was submersed in a water bath that is constantly cooled using a large copper coil connected to a chiller, stirred with a mixer, and refilled if needed by making use of a float valve. The test autoclave is connected to an accumulator to be used as a sCO₂ reservoir

and heated above the critical temperature. Thermocouples are placed in the accumulator, the water bath, and in the autoclave to monitor and record temperature changes. The pressure inside the autoclave and the accumulator is also recorded. The inside of the test autoclave depicts the insulation layers in dark yellow, the graphite susceptor inside the coil and the specimen holder in light yellow with stacked specimens in gray. A photograph of the test autoclave immersed in water is showed in Figure 4. The two insulated fittings used to connect the coil to the power head are on the left and the five-thermocouples tree is on the right.

To better replicate real life conditions, the specimens could not be placed inside the coil. The surface of the specimens would otherwise heat before heating the surrounding $s\text{CO}_2$. This would be an important issue for the TBC-coated specimens for which the temperature is expected to be lower on the substrate than in the environment. Furthermore, the different materials tested would not reach the same temperature at a fixed induction power and frequency since it is dependent on their individual electrical resistivity and magnetic property. Therefore, the decision was made to use a graphite susceptor in the coil to perform as a radiative and convective heat source to the specimens placed above the susceptor and outside the coil. A photograph of mockup test specimens placed on top of three graphite susceptor before being placed in the induction coil is showed in Figure 5. The susceptor and the specimen holder attached to the interior of the autoclave head with the induction coil present is shown before and after adding insulation in **Figure 6**. The specimen holder was a cylindrical piece of ceramic with seven through holes and a baseplate. The specimens were stacked on supporting Inconel wires and placed in the holes, see Figure 7.

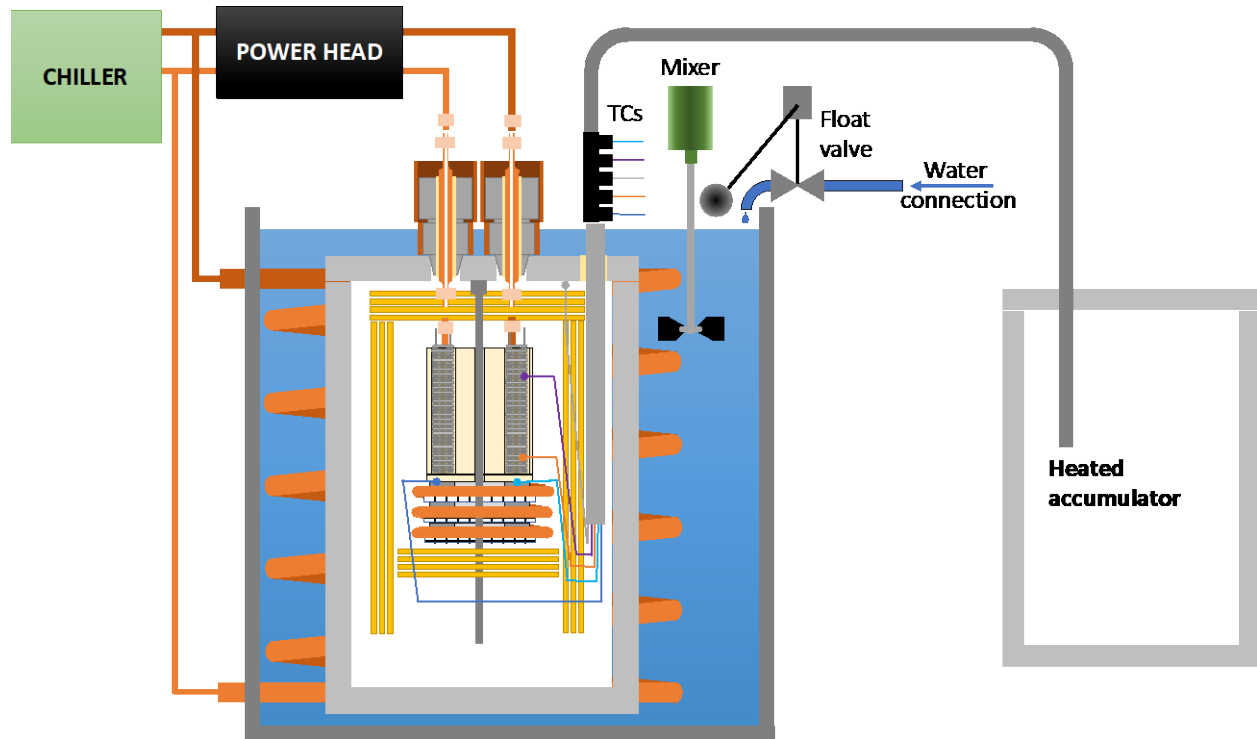


Figure 3. Schematic of induction heater test setup.



Figure 4. Photograph of the cooled autoclave immersed in water.



Figure 5. Photograph of four layers of stainless steel nuts (used as specimens mock-up) on top of three stacked 2.5" diameter graphite susceptors.

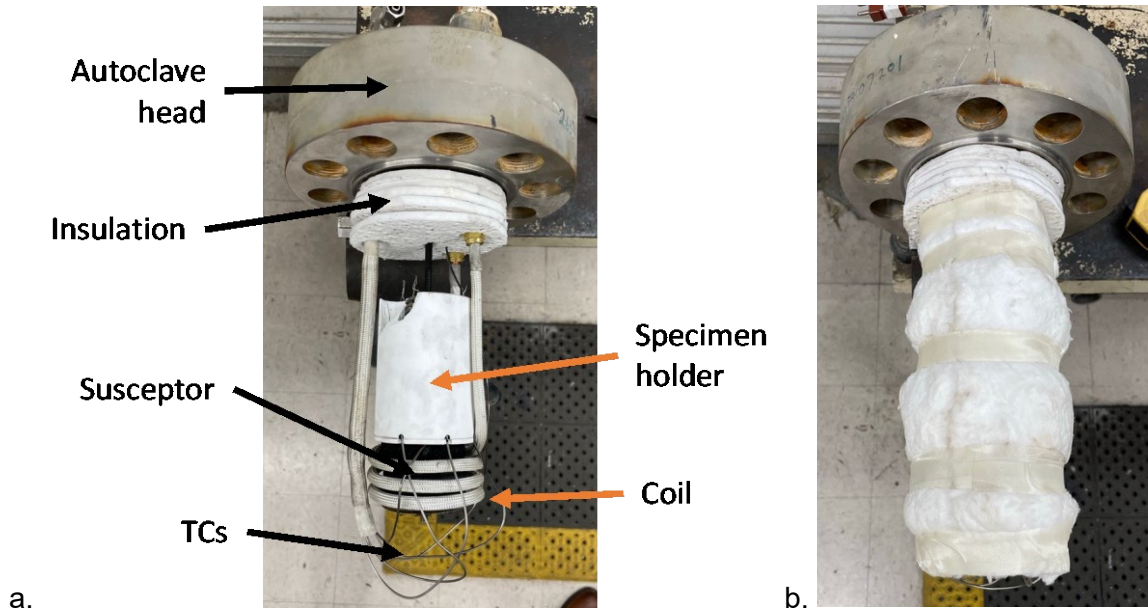


Figure 6. Photographs of the coil surrounding the graphite susceptor, the specimen holder, and the thermocouples a. before and b. after placing the insulation.

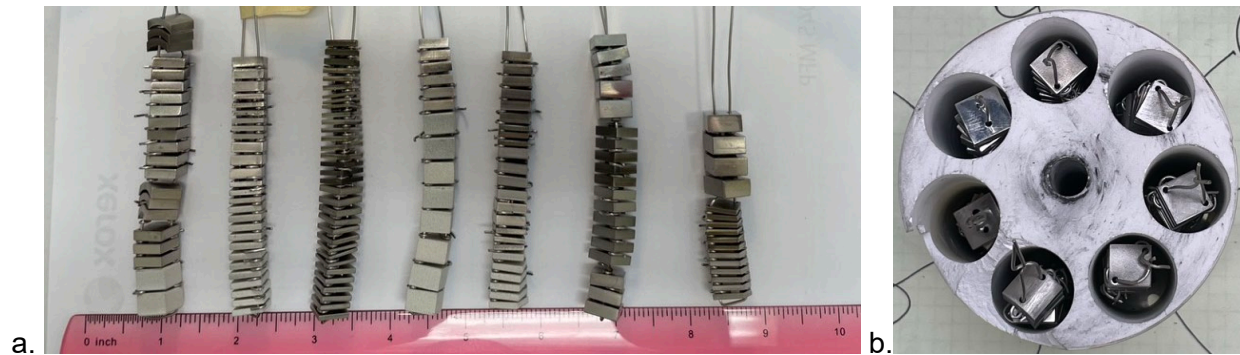


Figure 7. Photographs of a. the assembled specimens and b. the specimens placed in the vertical holes of the specimen holder.

Trial Run

Multiple trial runs have been performed and they have led to improvements across the whole system. An example of the temperature, pressure, and power data collected during one of those tests is shown in Figure 8. Temperatures were measured at two locations on the susceptor (“Susceptor 1” and “Susceptor 2”), and approximately 1.5” and 3” above the susceptor (“Mid” and “Top”). The pressure and the power applied (“Pw1”) as a percentage of the total power are included. The autoclave was pressurized with CO₂ at 1,489 psi at the beginning of the test to avoid phase change from occurring during the exposure. The power was controlled and raised manually, and the resulting temperature measured on the susceptor increased from ambient to 1,300 °C in less than 6 hours. The maximum pressure was 3,043 psi at 1,300 °C. At the same time, the temperatures measured near the mockup specimens varied between 700 °C and 1,000 C. This huge range of temperature indicates that radiative and convective heating of the

specimens using a graphite susceptor is inefficient. The large temperature gradients present in the test vessel (from 1,300 °C near the susceptor to less than 100 °C on the inside wall of the autoclave) result in large density variation (from ~70 kg/m³ near the susceptor to ~500 kg/m³ near the wall of the autoclave) that will lead to rapid convection that makes it difficult to maintain a constant high temperature. The maximum pressure and temperature measured so far in sCO₂ using the induction heater autoclave is compared in Figure 9 to the results reported in the literature by various other laboratories. Thus far, these trial runs have resulted in CO₂ pressures/temperatures that are higher than those that have been reported previously.

It was also observed that releasing CO₂ from the system increases the temperature at constant power, as shown in Figure 10. In the left half of the graph, a constant induction heating power was maintained, and CO₂ was released at regular interval. The pressure decreased from 2,075 psi to 1,625 psi, which led to a temperature increase of nearly 100 °C. For comparison, increasing the applied power by 5 point percentage resulted in an increase of 40 °C.

The failure of the graphite susceptor became a recurring issue after applying more than 75% of power. The susceptor did not appear to fail due to oxidation but it was mostly pulverized with some solid sections of the surface remaining. A photographic example is presented in Figure 11. Additional evaluation of the induction heating of graphite susceptor in ambient air and at high power was done by placing a 6" graphite rod on a steel carbon beam. The beam melted when 85% of power was applied on the graphite, despite being 3" away from the hot zone. This may indicate that the graphite temperature may exceed 2,000 °C, but the equipment required to measure those temperature was not available at the time. It is hypothesized that extremely high temperature was the cause the failure of the susceptor.

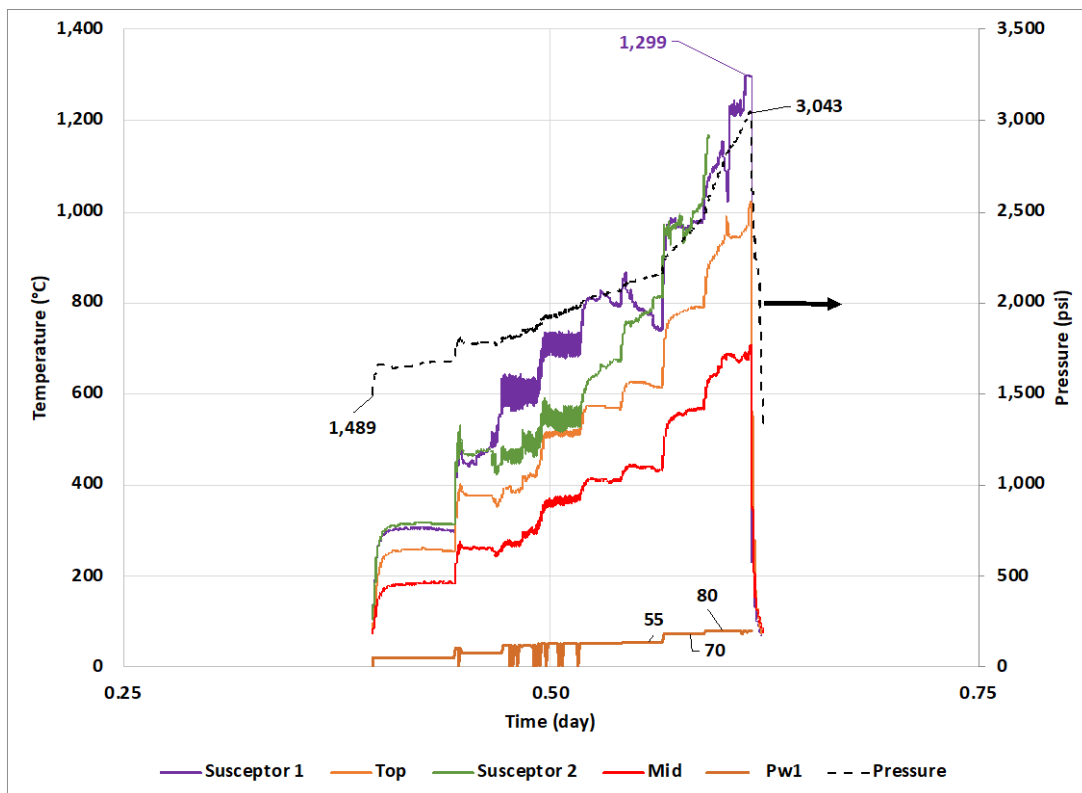


Figure 8. Example of the power applied, and the temperature and pressure measured inside the inductively heated autoclave.

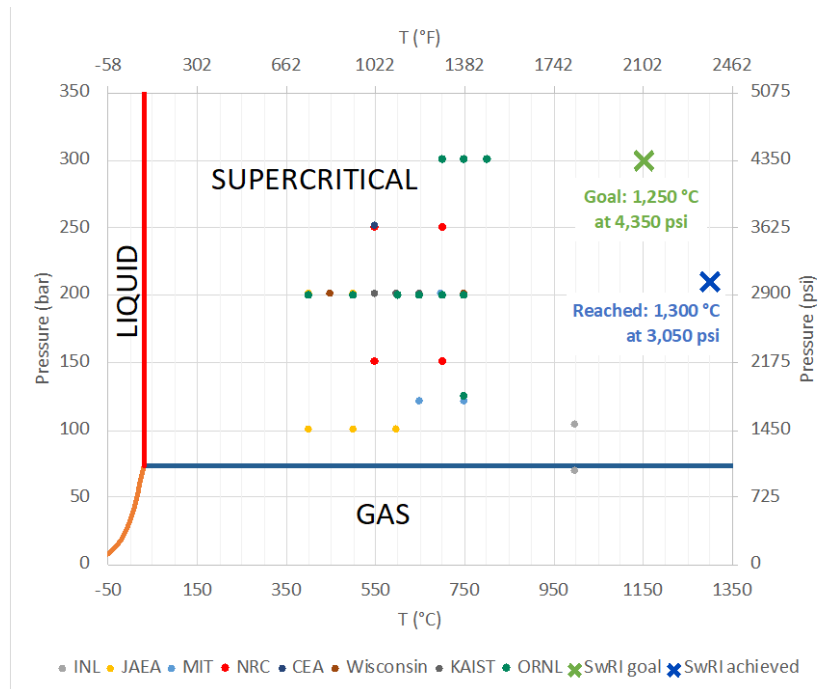


Figure 9. sCO₂ temperature and pressure achieved at SwRI compared to other laboratories.⁴⁻¹⁴

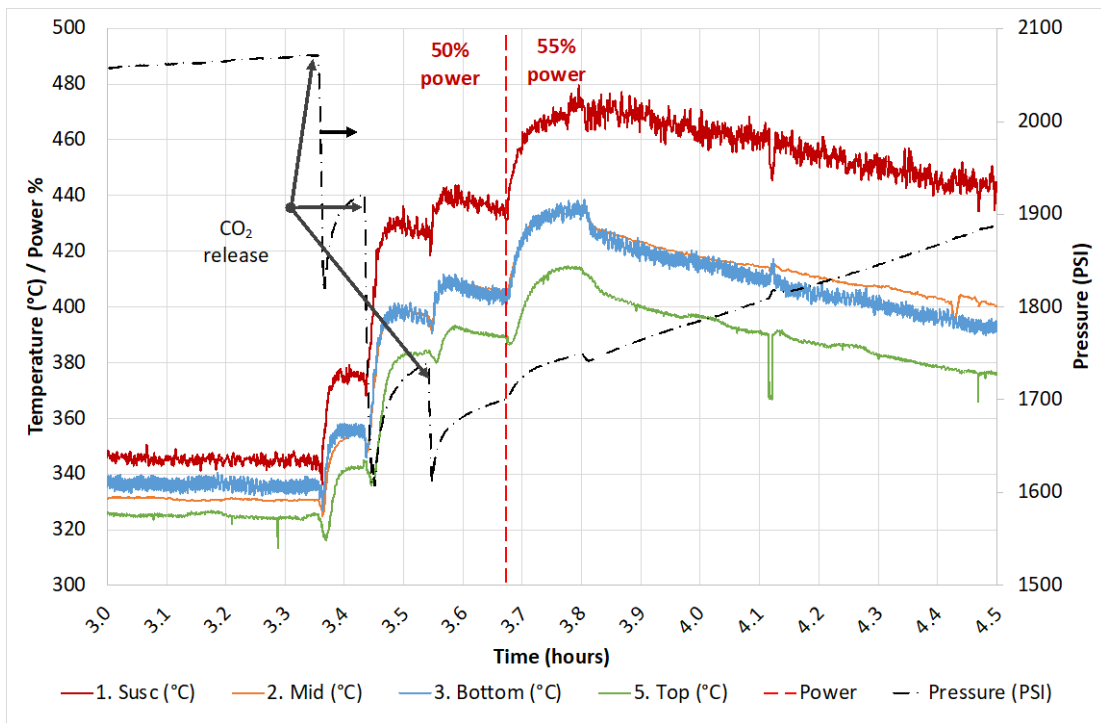


Figure 10. Measured temperature and pressure as a function of time and applied power during a period when CO₂ was released.



Figure 11. Failed graphite susceptor after high temperature exposure.

Optimizing Specimen Holder

The tests performed showed that it was possible to achieve temperatures higher than the test goal at pressure, but the heat transfer was suboptimal and most of the specimens would not be exposed to $s\text{CO}_2$ exceeding $1,000\text{ }^\circ\text{C}$. It was decided to review and revise the design of the specimen holder and susceptor assembly. The goal was to rely more on heat transfer through the assembly and less on radiative and convection heating. The specimen holder and the susceptor are combined in a single block. The specimens are placed in vertical holes above and below a 1.25" thick susceptor section. A lid and a baseplate are added to increase the efficiency of the setup by limiting the escape of hot $s\text{CO}_2$. A schematic of the design is showed in Figure 12. After reviewing multiple high temperature alloys and materials, it was decided to use stainless steel 310 because of its good combination of resistivity and magnetic properties (for induction heating), ease of sourcing and machining (compared to other materials such as tungsten and titanium), and suggested maximum service temperature ($1150\text{ }^\circ\text{C}$ for 310 stainless steel compared to $925\text{ }^\circ\text{C}$ for 316 stainless steel). Modeling of the thermal diffusion and the resulting stresses were performed.

The thermal model assumed that the susceptor section would heat to $1250\text{ }^\circ\text{C}$ on the surface while the nearby environment is at $700\text{ }^\circ\text{C}$. A variable temperature was assigned to the outer midsection surface to simulate induction heating. For the external surface outside of coils, natural convection coefficient was used based on concentric cylinders equation. For internal surfaces, an estimated $0.25\times$ factor of natural convection coefficient was used. This was chosen based on the assumption that the flow is restricted by the lid. The results of the thermal model are showed in Figure 13. The temperature in the specimen holding vertical holes was found to vary between $1,110\text{ }^\circ\text{C}$ to $1,190\text{ }^\circ\text{C}$.

The structural model assumed a zero axial displacement at the top of a cylinder attached to the lid (equivalent to the all-thread used in the autoclave) and tangential support to restrict rotation. These are necessary constraints to obtain a solution. The results are presented in Figure 13. Using literature data for the elastic modulus of 310 stainless steel at high temperatures, stress levels for elastic-only model are close to the UTS in this temperature range. This indicates that there may be some local plastic deformation but likely not enough to cause failure.

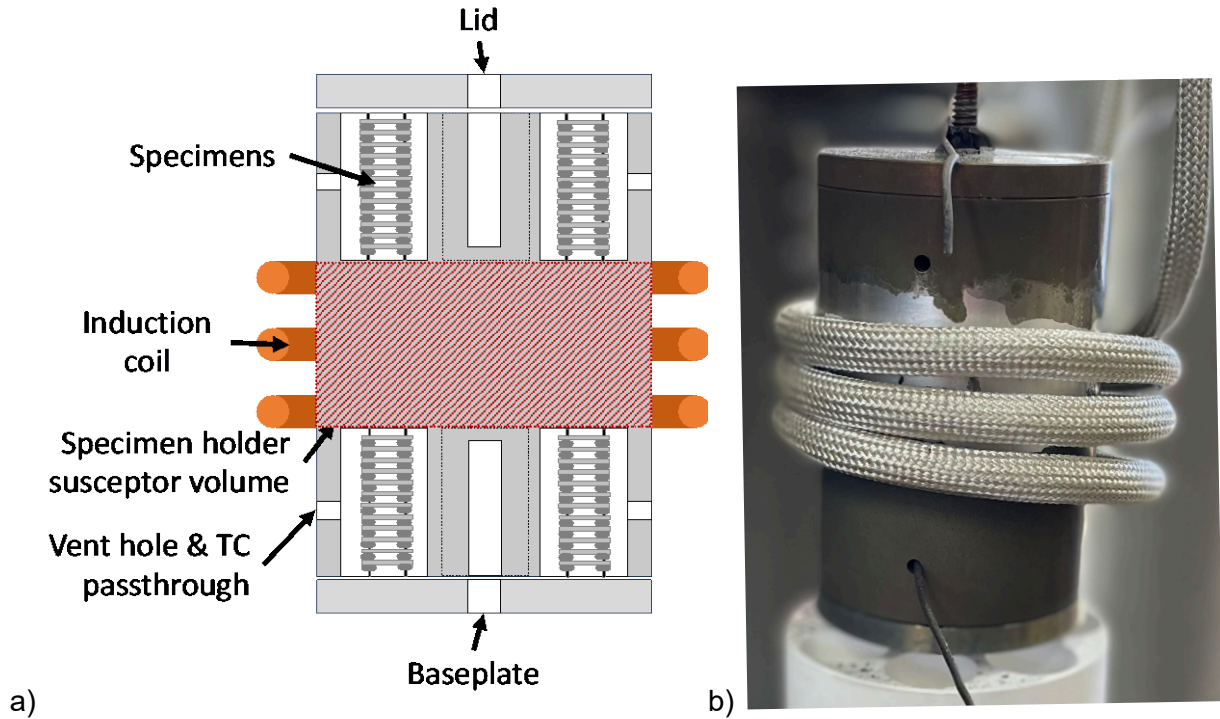


Figure 12. a) Cross sectional schematic and b) photograph of the optimized design of the specimen holder/susceptor assembly inside an induction coil (in orange).

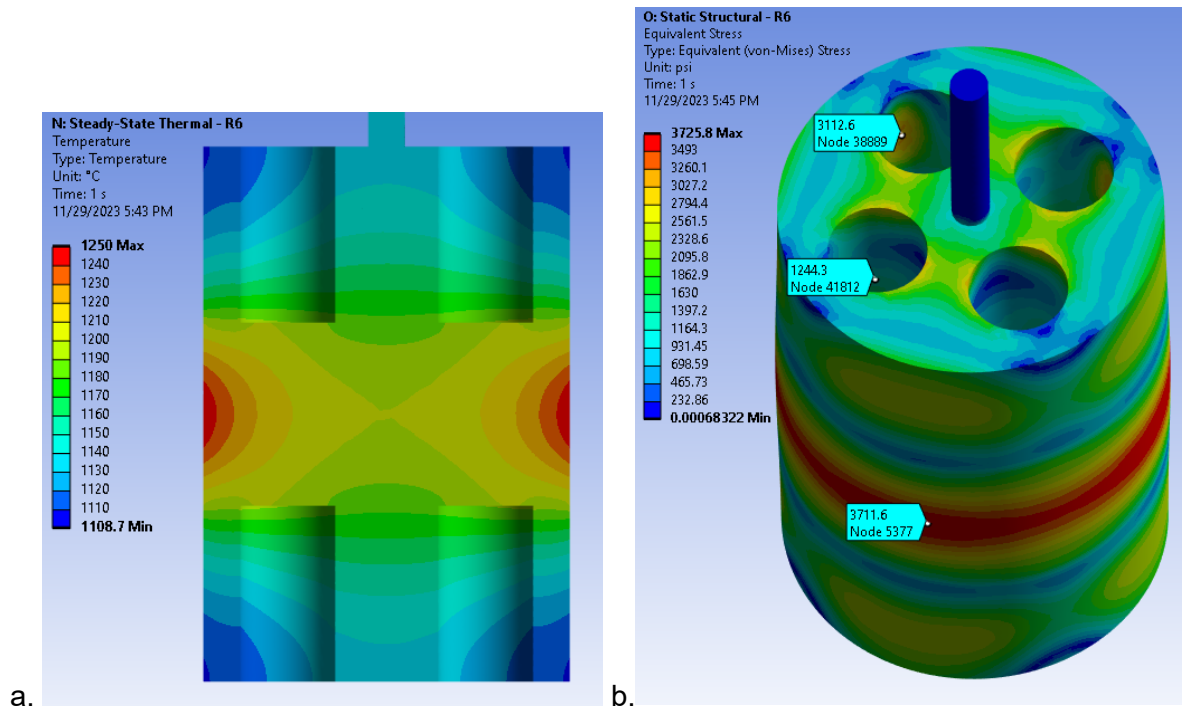


Figure 13. a. Thermal and b. structural model of the optimized specimen holder design.

CONCLUSION

The unique testing facility necessary to test materials in sCO₂ conditions similar to those expected in the first stages of a direct-fired sCO₂ turbine was accomplished. Throughout multiple tests, it was confirmed that temperatures well above 1,000 °C could be reached under pressure above 3,000 psi. High pressure and temperature were successfully maintained for days. However, relying on convection and radiation to transfer heat from a remote graphite susceptor to the specimens was not efficient as temperature drop of 500 °C were measured over approximately 3". The power required to try to reach the goal temperature of 1,250 °C on the specimens resulted in recurring failures of the graphite susceptors. Using a combined susceptor and specimen holder will permit to use heat diffusion through a single metallic alloy block. Preliminary thermal and structural modeling of a single block design confirms that less than 100 °C variation may be achieved and that the thermal stresses are not expected to damage the new design.

REFERENCES

1. Weiland, N. T. & White, C. W. *Performance and Cost Assessment of a Natural Gas-Fueled Direct sCO₂ Power Plant*. NETL-PUB--22274, 1503567 <http://www.osti.gov/servlets/purl/1503567/> (2019) doi:10.2172/1503567.
2. Goff, A., Lu, X. & Fetvedt, J. *Allam Cycle Zero Emission Coal Power*. (2020).
3. Moore, J. *et al.* Development of a 300 MWe Utility Scale Oxy-Fuel sCO₂ Turbine. in *Proceedings of ASME Turbo Expo 2023* (2023).
4. Pint, B. A. & Keiser, J. R. The Effect of Temperature on the sCO₂ Compatibility of

- Conventional Structural Alloys. in *Proceedings of the 4th International Symposium on Supercritical CO₂ Power Cycles*. (2014).
5. Pint, B. A. & Thomson, J. K. Effect of Oxy-Firing on Corrosion Rates at 600–650 °C. *Materials and Corrosion* **65**, 132–140 (2014).
 6. Pint, B. A., Brese, R. G. & Keiser, J. R. Effect of Pressure on Supercritical CO₂ Compatibility of Structural Alloys at 750 °C. *Materials and Corrosion* **68**, 151–158 (2017).
 7. Pint, B. A., Brese, R. G. & Keiser, J. R. Supercritical CO₂ Compatibility of Structural Alloys at 400-750C. in *Corrosion 2016* (NACE International, 2016).
 8. Kung, S. C. *et al.* Oxidation/Corrosion in Materials for Supercritical CO₂ Power Cycles. in *Proceedings of the 5th International Symposium on Supercritical CO₂ Power Cycles*. (2016).
 9. Kung, S. C., Shingledecker, J. P., Wright, I. G. & Tossey, B. M. Oxidation and Carburization of Alloys Exposed to Impure Supercritical CO₂. in *Corrosion 2017* (NACE International, 2017).
 10. Cao, G., Firouzdar, V., Sridharan, K., Anderson, M. & Allen, T. R. Corrosion of Austenitic Alloys in High Temperature Supercritical Carbon Dioxide. *Corrosion Science* **60**, 246–255 (2012).
 11. He, L.-F. *et al.* Corrosion Behavior of an Alumina Forming Austenitic Steel Exposed to Supercritical Carbon Dioxide. *Corrosion Science* **82**, 67–76 (2014).
 12. Jelinek, J. J. *et al.* Corrosion Behavior of Alloys In High Temperature Supercritical Carbon Dioxide. in *Corrosion 2012* (NACE International, 2012).
 13. Roman, P. J. *et al.* Corrosion Study of Candidate Alloys in High Temperature, High Pressure Supercritical Carbon Dioxide for Brayton Cycle Applications. in (NACE International, 2013).
 14. *Fundamentals and Applications of Supercritical Carbon Dioxide (SCO₂) Based Power Cycles*. (Woodhead Publishing, 2017).

ACKNOWLEDGEMENTS

This material is based upon work supported by the U.S. Department of Energy under Award Number DE-FE0031929.

The authors wish to acknowledge Justin Been (SwRI) for his assistance in building the high pressure and high temperature induction test setup and performing the testing, and Dustin Noll (SwRI) for his assistance in measuring and photographing the test specimens.

Ray Ariss, of Inductronix, is thanked for his continuous help and support in uniting the induction heater to the autoclave and in troubleshooting the entire system.

The assistance of Steve McCoy and Jack deBarbadillo of Special Metals, of Brett Tossey and Vinay Deodeshmukh of Haynes International, and of Luiza Esteves of Sandvik in providing the test materials is also acknowledged.

Plasma Technology, Inc. is recognized for the depositions of the thermal spray bond coat and the thermal barrier coatings.

DISCLAIMER

This report was prepared as an account of work sponsored by an agency of the United States Government. Neither the United States Government nor any agency thereof, nor any of their employees, makes any warranty, expressed or implied, or assumes any legal liability or responsibility for the accuracy, completeness, or usefulness of any information, apparatus, product, or process disclosed, or represents that its use would not infringe privately owned rights. Reference herein to any specific commercial product, process, or service by trade name, trademark, manufacturer, or otherwise does not necessarily constitute or imply its endorsement, recommendation, or favoring by the United States Government or any agency thereof. The views and opinions of authors expressed herein do not necessarily state or reflect those of the United States Government or any agency thereof.